SECOND EUROPEAN CONFERENCE ON EARTHQUAKE ENGINEERING
AND SEISMOLOGY, ISTANBUL AUG. 25-29, 2014

SEISMIC RESPONSE OF TUNNEL SHAFTS

Juan M. MAYORAL[1], Neftalí SARMIENTO[2] and Ernesto CASTAÑON[3]

ABSTRACT

There is a lack of information regarding the seismic response of tunnel shafts. Seismic-induced stresses in the shaft do not only depend on the ground motion and the soil characteristics but also are affected by the relative stiffness between the soil and the shaft structure. In this paper, a numerical study of the seismic response of typical tunnel shafts commonly used in Mexico City drainage systems is presented. The work is aiming at establishing the controlling design seismic parameters of the shaft. It is assumed that the shafts have a varying depth from 22 to 34m, and external diameters ranging from 12 to 16m, and are located in the very soft high plasticity clay of the former Texcoco Lake located in the surroundings of Mexico City valley, which exhibits low strength and high compressibility. Series of 3D finite differences models were developed in order to simulate the dynamic response of shafts, subjected to a typical subduction earthquake scenario, generated in the Pacific Coast, developed for a return period of 475 years. The ground motion was deconvolved to the base of the soil deposit, and applied to the 3D models as an acceleration time history and quiet boundaries were used in order to avoid reflection of propagating waves back into the model. From the results gathered from this study insight was gained regarding the seismic response of shafts.

INTRODUCTION

Failures observed in hydraulic underground strategic infrastructure during recent seismic events such as Loma Prieta, 1989; Kobe, 1995; Kocaeli and Duzce, 1999; Chi-Chi, 1999 and Mid-Niigata, 2004 earthquakes have clearly shown that the seismic behaviour of these structures is far from being fully understood. In particular, there is a lack of information regarding the seismic response of shafts. Seeking to build both safe and economical structures, the engineer must be able to quantify accurately the input loading, to evaluate properly the soil behaviour under this loading (Safak, 2001; Darendeli, et al., 2001; Dobry et al.,1987), and to make reliable assessments of the soil–shaft system response (Amorosi et al., 2009 and Wang et al.; 2001). This is particularly important when considering large return periods for the seismic event (eg. 475 years for the Operating Basis Earthquake, and 2475years for the Maximum Credible Earthquake), these seismic demands, combined with the large ground movement amplifications expected to occur in the high plasticity clays found in the Mexico City valley, which exhibit a very large linear range in their modulus degradation an damping curves, should be taken explicitly during the shaft seismic design. Seismic loading acting upon a soil-shaft system is the result of the interplay of earthquake incoming waves with the structure stiffness.

In this paper, sets of three-dimensional finite difference models were developed in order to simulate the dynamic response of shafts, subjected to a typical subduction earthquakes scenario,

[1] Researcher Institute of Engineering, UNAM Mexico City, JMayoralV@iingen.unam.mx
[2] Researcher Institute of Engineering, UNAM Mexico City, NSarmientoS@iingen.unam.mx
[3] Graduate student Institute of Engineering, ECastanonL@iingen.unam.mx

generated in the Mexican Pacific Coast, developed for a return period of 475 years. The ground motions were deconvolved to the base of the soil deposit, and applied to 3D models as an acceleration time history and quiet boundaries were used in order to avoid reflection of propagating waves back into the model. From the results gathered herein, a better understanding of the factors controlling the seismic response of shafts was established.

SUBSOIL CONDITIONS

Typical subsoil conditions found at the former Texcoco Lake has been studied by several researchers (Mayoral et al., 2008a; Osorio and Mayoral, 2013 and Mayoral et al., 2014), commonly the soil profile at this zone presents a desiccated crust of clay at the top extending up to a depth of 1.0 m, which is underlain by a soft clay layer approximately 38 to 66m thick, with interbedded lenses of sandy silts and silty sands. The plasticity index ranges from 87 to 293%. Underneath this elevation, a competent layer of very dense sandy silt is found. The distance from the National University of Mexico, CU, to the polygon center that encloses the studied area is approximately 25.90km. The region studied is instrumented with four seismic stations, TXSO, TXS1, TXS2 and TXCH. A fifth station used in the analysis, TXRC, is located to the east, on a rock outcrop, about 19.20km (Fig. 1) away from the studied site.

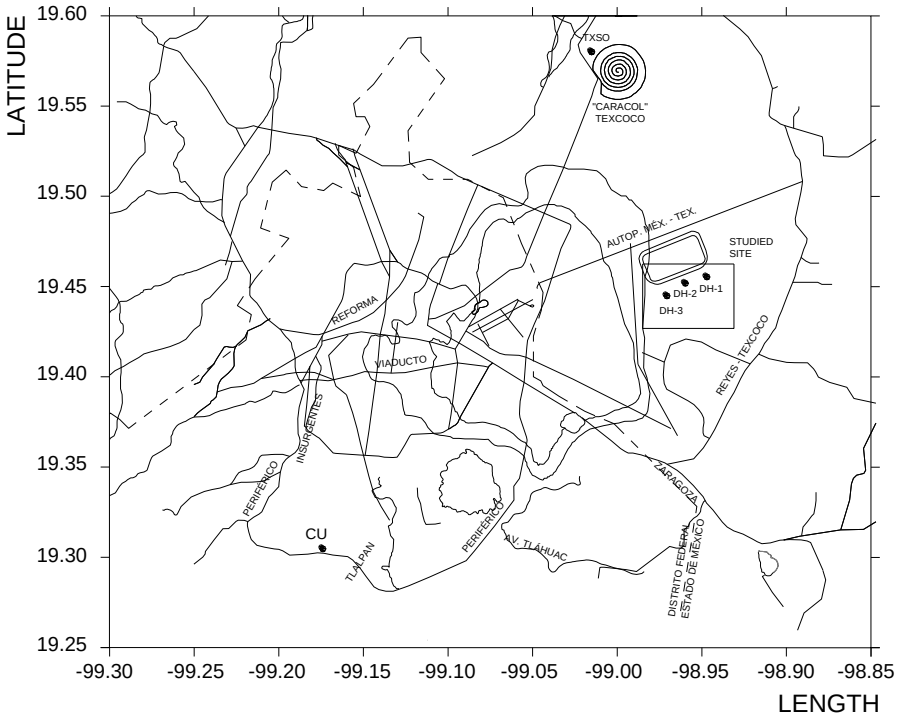

Figure. 1 Location of the studied area

Shear wave velocity determination

A generic shear wave velocity, Vs, profile have been established based on research conducted in the area mainly comprised by down-holes tests and ambient noise measurements (Mayoral et al., 2014), and empirical approaches based on empirical relationships between the tip cone penetration resistance and the shear wave velocity, V_s (Romo and Ovando, 1991). The idealized geotechnical section for analysis included herein is presented in Fig. 2, which also shows the shear wave velocity distributions with depth obtained from down-hole tests, DH.

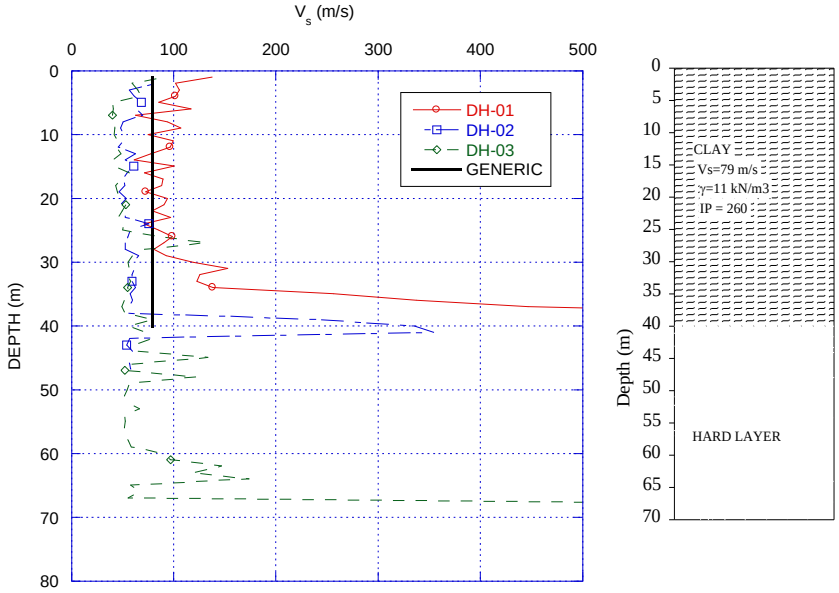

Figure. 2 Generic profile and shear wave velocity profiles measured from down hole-tests, DH

DYNAMIC PROPERTIES

Modulus degradation and damping curves can be obtained through laboratory testing in undisturbed soil samples, or empirical models function of soil type and other variables. In this research, due to the lack of experimental data, the empirical model proposed by Darendeli and Stokoe (2001), were used to generate modulus degradation and damping curves, which take into account confining pressure effects, σ´, plasticity index, PI, over consolidation ratio, OCR, the frequency of loading, f, and the number of loading cycles, N. This model is given by the following relationships:

$$\frac{G}{G_{\max}} = \frac{1}{1+\left(\frac{\gamma}{\gamma_r}\right)^a} \tag{1}$$

$$\gamma_r = \left(\phi_1 + \phi_2 PI(OCR)^{\phi_3}\right)\sigma'^{\phi_4} \tag{2}$$

$$\lambda = \lambda_{\min} + b\left(\frac{G}{G_{\max}}\right)^{0.1}\lambda_{msg} \tag{3}$$

$$\lambda_{msg} = c_1 + \lambda_{msg,a=1.0} + c_2\lambda_{msg,a=1.0}{}^2 + c_3\lambda_{msg,a=1.0}{}^3 \tag{4}$$

$$\lambda_{msg,a=1.0} = \frac{100}{\pi}\left[4\frac{\gamma - \gamma_r \ln\left(\frac{\gamma+\gamma_r}{\gamma_r}\right)}{\frac{\gamma^2}{\gamma+\gamma_r}} - 2\right] \tag{5}$$

where a=0.9190 (curvature coefficient), b=0.620 (scaling coefficient), γ is the shear strain (%), γ_r is a reference shear strain, σ'=effective confining stress (atm), λ_{min} is damping ratio at small deformations, λ_{msg} is the massing damping, and $\lambda_{msg,a=1.0}$ is the damping for a=1.0. The model coefficients are given by:

c1=-1.1143*a2+1.8618*a+0.2523
c2=0.0805*a2-0.0710*a-0.0095
c3=-0.0005*a2+0.0002*a+0.0003
ϕ1=0.0352,ϕ2=0.001,ϕ3=0.3246,ϕ4=0.3483,ϕ6=0.801,ϕ7=0.0129,ϕ8=-0.107,ϕ9=-0.289

For this research work, the curves proposed by Darendeli and Stokoe (2001) were deemed appropriated because they can be used for sands and clays, taking into account explicitly the most important factors that can influence the dynamic soil behaviour. To obtain the modulus degradation and damping curves, the over consolidation ratio, OCR, was taken as one, considering that the studied zone is located in the virgin former Texcoco lake, and that the over consolidation of the soil due to desiccation occurred only in the first couple of meters. Thus, changes in the seismic response of the soil deposit due to this fact are expected to be negligible. In this manner, the definition of the modulus degradation and damping curves results in only a function of plasticity index, PI. In this particular case, an average value of PI of 260 % was considered for the generic soil deposit (Fig. 3).

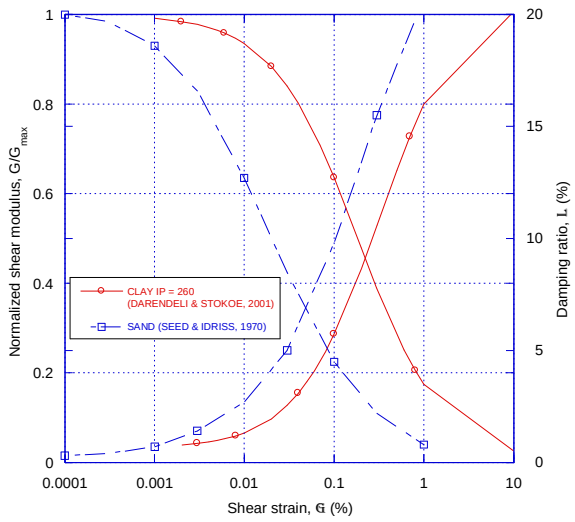

Figure. 3 Modulus degradation and damping curves used in the analyses

SEISMIC ENVIRONMENT

The seismic environment at the studied site was characterized through a probabilistic seismic hazard analysis, PSHA. In general, the steps needed to conduct a probabilistic seismic hazard analysis are (1) identification of all earthquake sources capable of producing damaging ground motions (2) characterization of the earthquake recurrence model, (3) definition of the attenuation relationship, (4) calculation of seismic risk and uniform hazard response spectrum, and (5) computation of deaggregation of the probabilistic seismic risk (Sabetta et al., 2005; Romeo et al., 2000 and Mayoral and Osorio, 2013).

The uniform hazard spectrum determined to characterize the seismic environment for the subduction seismogenic zone of the Mexican pacific Coast, was developed at the same location as the rock station TXCR, at about 18.70 km from the site, to be able to compare it directly with measured responses. As it is well known, the uniform hazard spectra, UHS, is a representation of the relationship between the natural vibration period, T, and spectral acceleration, Sa, for a given exceedance probability associated with a return period. Uniform hazard spectra for return periods 125, 250, 475, 2475 years was obtained from the seismic hazard curves, see Fig. 4. Note that this spectrum defines the seismic environment of the area. Therefore, it was used as input motion during the site response analyses.

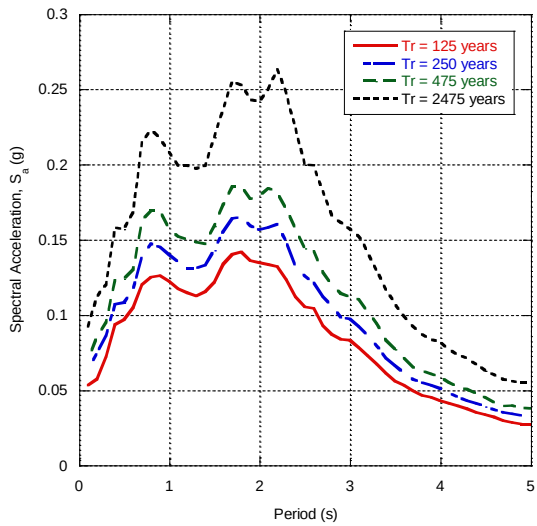

Figure. 4 Computed uniform hazard spectra for four return periods at TXCR

Synthetic accelerogram

To develop time histories which response spectra reasonably match the design response spectrum, the selected (recorded) time histories were modified using the method proposed by Lilhanand and Tseng (1988) as modified by Abrahamson (1993). This approach is based on a modification of an acceleration time history to make it compatible with a user specified target spectrum. The adjustment of the time history can be performed with a variety of different modification models. In doing so, the long period non-stationary phasing of the original time history is preserved. The 5% damped response spectra calculated for the modified time histories are compared. The seed and synthetic ground motions are shown in Fig. 5, and the corresponding response spectra are shown in Fig. 6. It can be seen that the response spectra calculated from the modified time histories reasonably match the target spectrum.

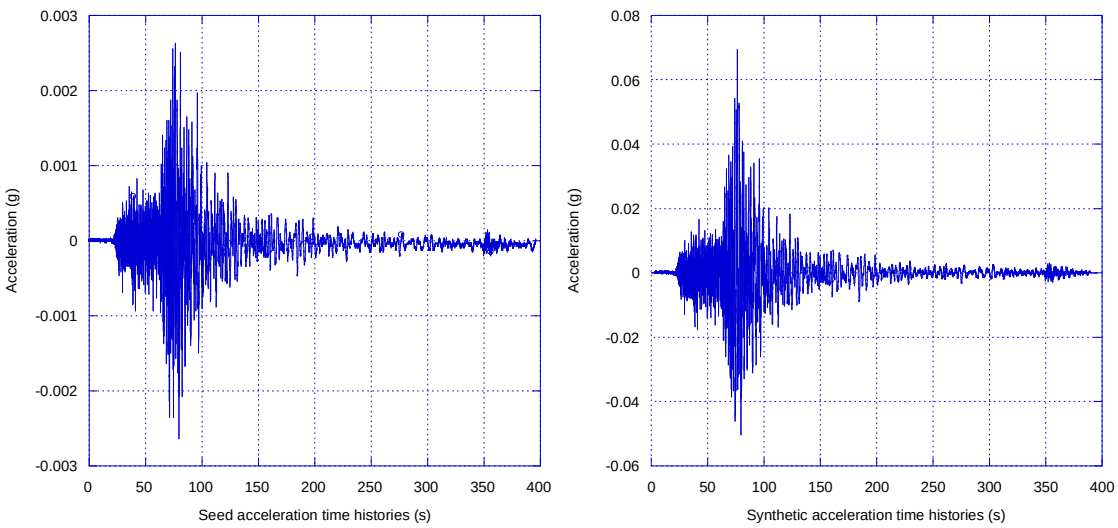

(a) (b)

Figure. 5 Seed (a) and synthetic (b) time histories

SITE RESPONSE ANALYSIS

Considering the well-defined relative shallow horizontally layered geological structure found at the site during the subsurface characterization, a 1-D wave propagation analysis was considered

appropriate to reproduce with reasonable accuracy, recorded ground motions (Rosenblueth, 1952; Idriss et al., 1968; Romo, et al., 1986; Seed et al., 1994). Accordingly, to find the ground motions in rock to be used in time domain soil-structure interaction analyses, time histories computed at the ground surface were deconvolved to the stiffer materials found at the base of the soil profile.

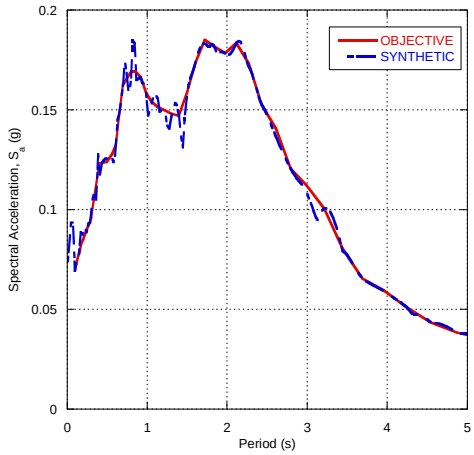

Figure. 6 Objective and synthetic ground motion response spectra

The computer code SHAKE (Schnabel et al., 1972), which solves the wave equation for SH waves propagating vertically in the frequency domain, was used for this task. Equivalent linear properties were deemed appropriate to represent soil nonlinearities, considering the high plasticity exhibited by the clay at the site. This is supported by the fact that there is not a significant enlargement of the predominant period or attenuation of the spectral ordinates observed in response spectra of recordings registered at station TXSO for events with Ms larger than 5, even for the destructive 1985 event. The analysis is done in the frequency domain, and, therefore, for any set of properties it is a linear analysis. An iterative procedure is used to account for the nonlinear behaviour of the soils.

SEISMIC SOIL-STRUCTURE INTERACTION, SSSI, ANALYSIS

The seismic analysis was carried out with a fully dynamic 3-D analysis performed with the program FLAC^{3D}. The tridimensional finite difference model of the free field was calibrated against the results obtained with the program SHAKE, which, in turn, has been extensively calibrated against theoretical and experimental data. The shaft was modelled with solid element. The shaft was modelled with s, will have 240, 288, 336 and 384 solid elements for the depths of 20, 24, 28 and 32 respectively. The shaft wall thickness is 0.80m. The damping of these structural elements is 5%. The concrete properties are compiled in Table 1. The FLAC3D mesh has a total of 6240 zones and 6573 nodal points. The model base is a square four times the shaft diameter, D. The model depth is 40m in all cases (Fig. 7). An elasto-plastic Mohr–Coulomb model was used to represent the stress–strain relationship for soils. The calculation is based on the explicit finite difference scheme, to solve the full equations of motion, using lumped grid point masses derived from the real density of surrounding zones (rather than fictitious masses used for static solution). This formulation can be coupled to the structural element model, thus permitting analysis of soil structure interaction.

Table. 1 Concrete properties used in the analysis

Parameter	Value	Units
Strength at 28 days, f'c	35	MPa
Young modulus at 28 days, Ec	26,000	MPa
Poisson ratio, υ_c	0.2	-

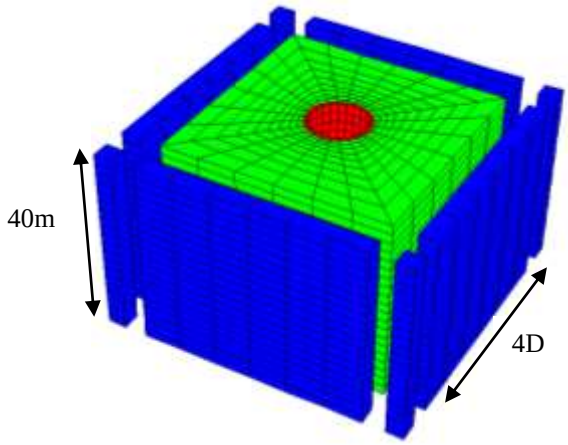

Figure. 7 Tridimensional finite difference model

Analysis Results

Figures 8 shows an schematic representation of the shaft showing the points were acceleration and displacement time histories were computed for the case where the shaft diameter, D, was 12m and the shaft high, H, was 32m. The corresponding acceleration time histories in the shaft, near field, and free field at the surface, are presented in Fig. 9. These histories were also computed at four elevations 0, -16, -32 and -40m in the shaft, near field, and far field. Figures 10 and 11 showed the corresponding acceleration and displacement time histories at the same elevations in the shaft and near field.

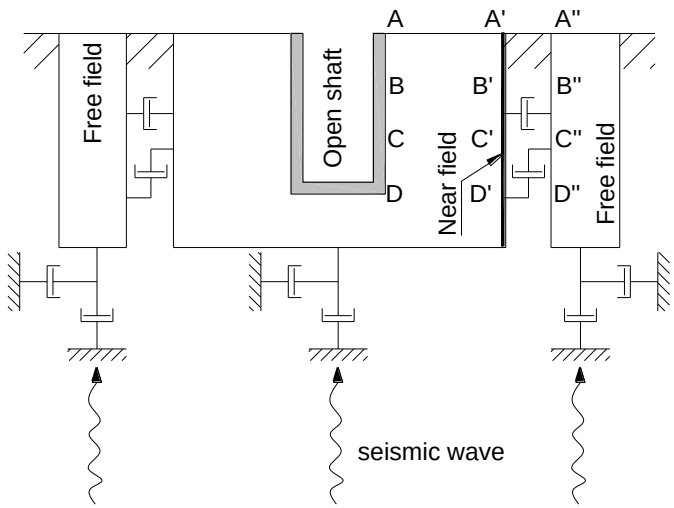

Figure. 8 Numerical model schematic representation and control point locations

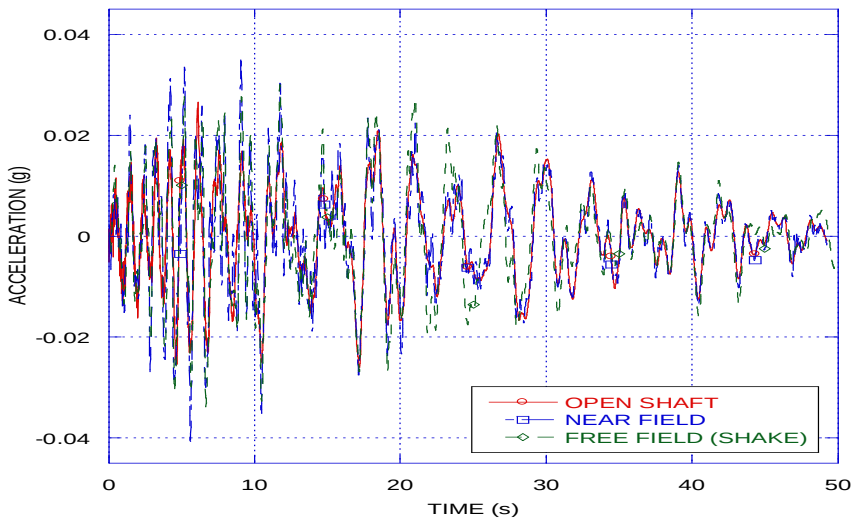

Figure. 9 Computed response at the shaft, near field and free field at the surface

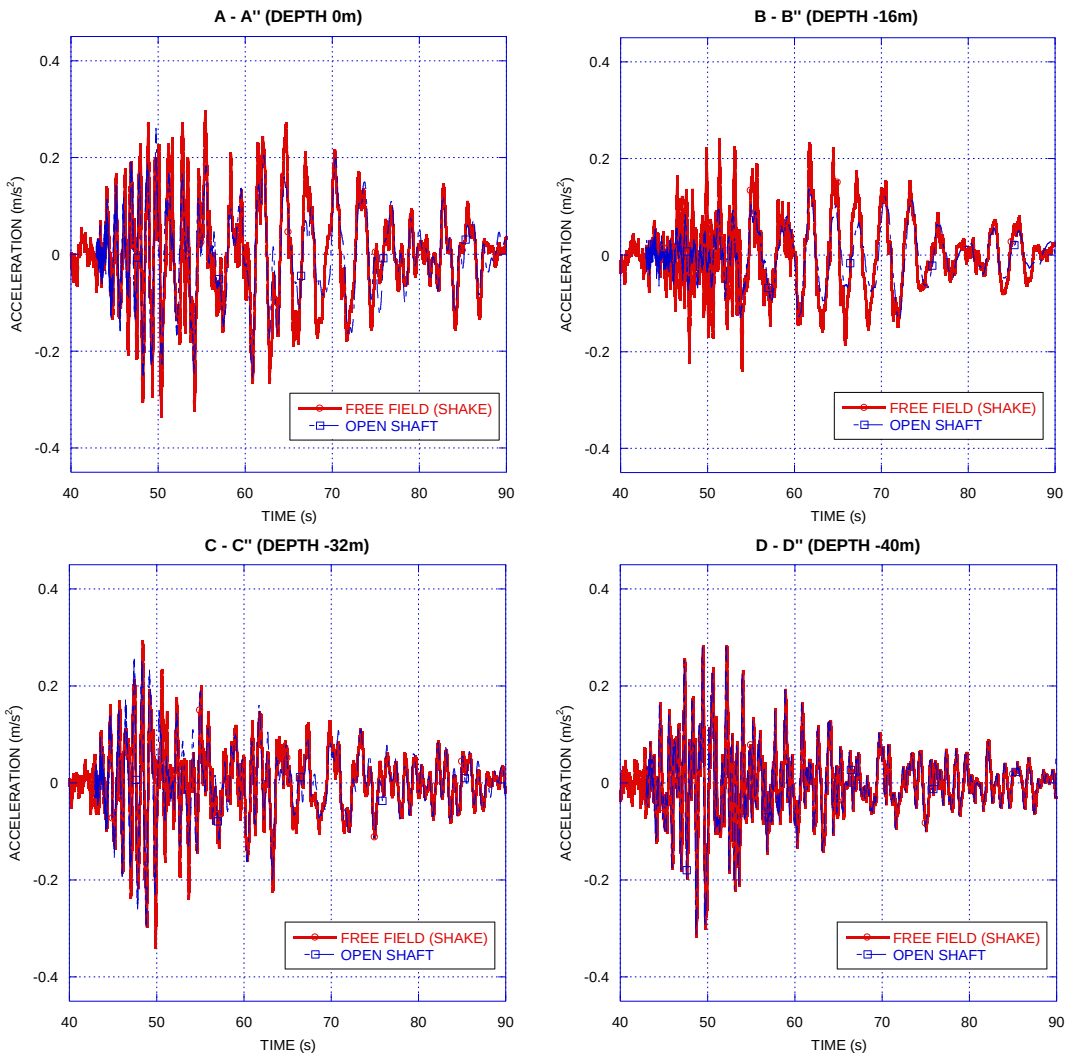

Figure. 10 Acceleration histories at th shaft, near field and free field

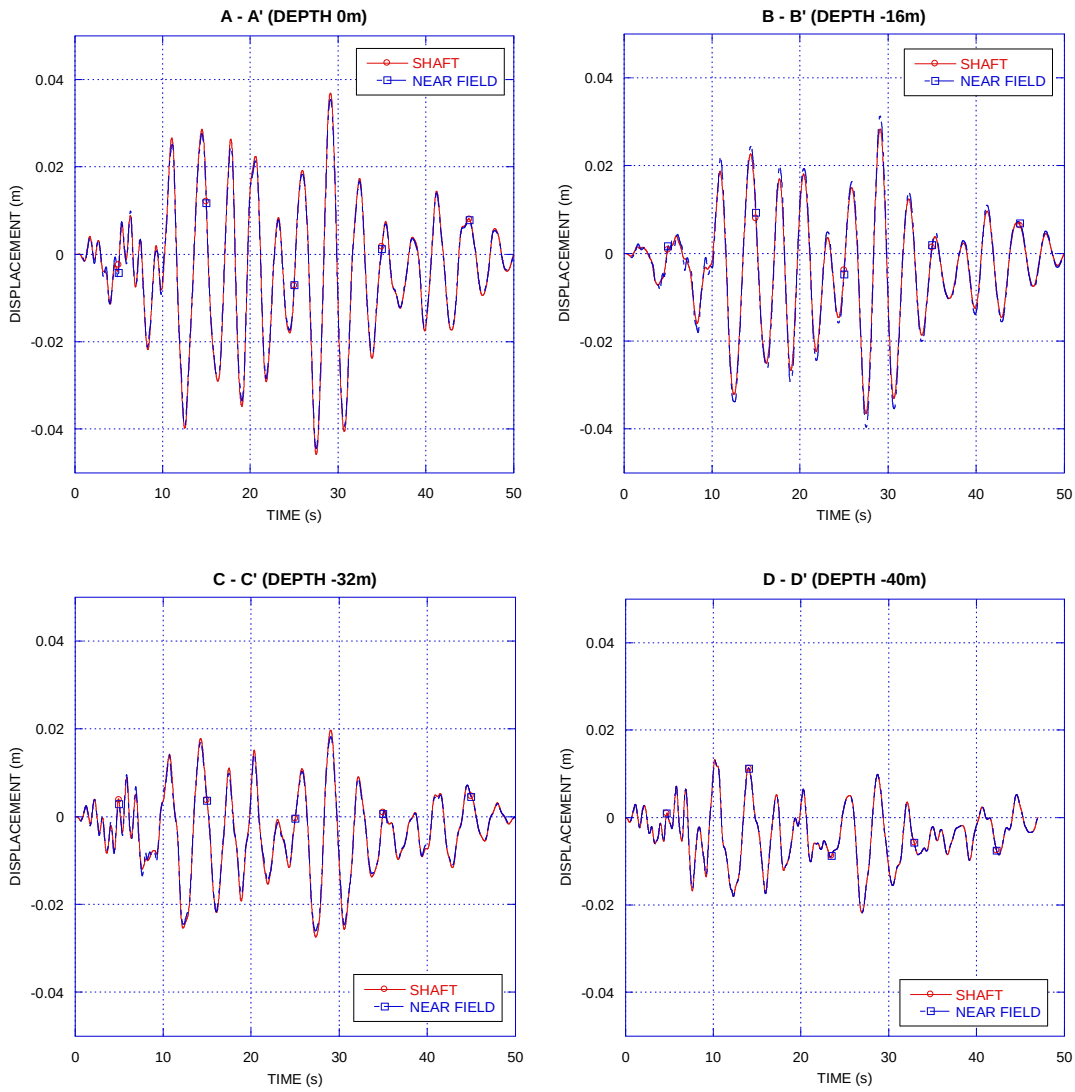

Figure. 11 Displacement time histories at the shaft and near field

Figure 12 shows the maximum accelerations and displacements computed in the shaft and the free field for all cases. As can be noticed the shaft moves as a rigid body. The difference between the free filed motions and the shafts motions generates compressive and tensile stresses in the shaft. Figure 13 shows the corresponding octahedral stress computed with the expression Eq. (6), for the time where the maximum displacement occurs (i.e t=22s).

$$\tau_{oct} = \frac{\sqrt{((\sigma_1 - \sigma_2)^2 + (\sigma_2 - \sigma_3)^2 + (\sigma_3 - \sigma_1)^2}}{3} \qquad (6)$$

where σ_1, σ_2 and σ_3 are the principal stresses.

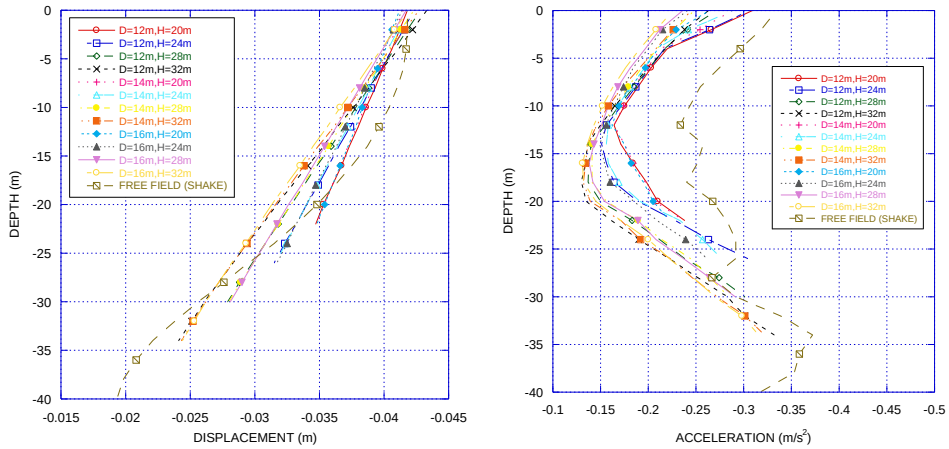

Figure. 12 Computed maximum displacements and accelerations in the shaft and free field

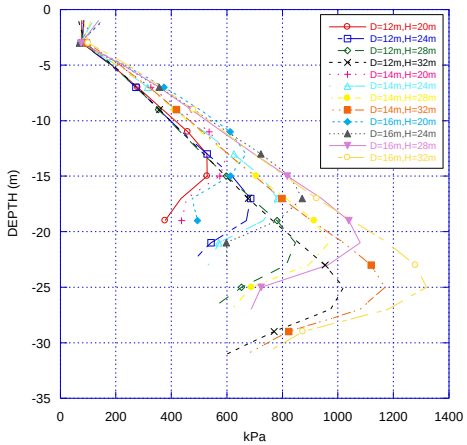

Figure. 13 Computed seismic-induced octahedral stresses

The corresponding horizontal and vertical stresses along with the major and minor principal stresses are presented in Figs. 14 and 15 respectively.

Horizontal stress Vertical stress

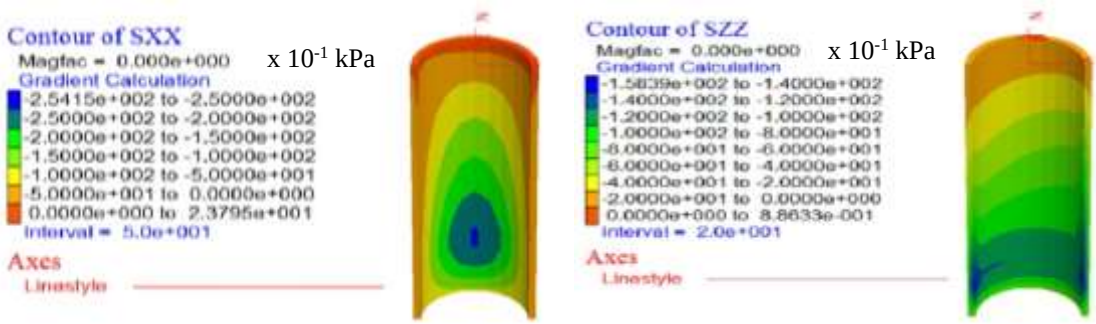

Figure. 14 Horizontal and vertical stresses

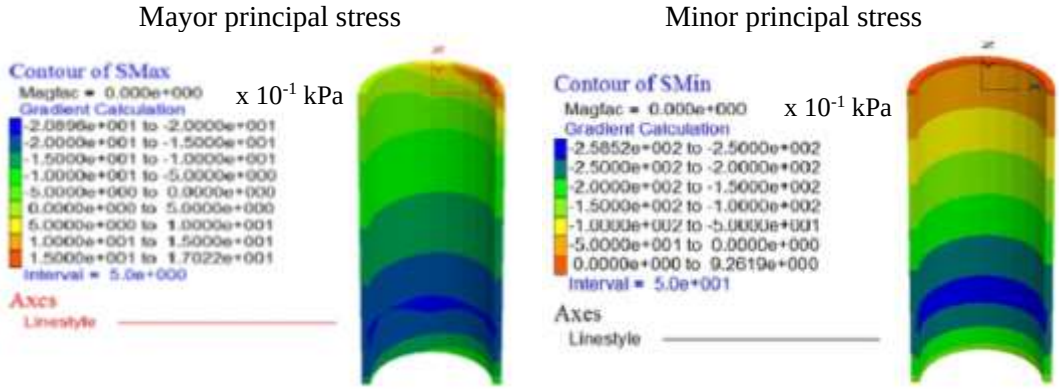

Figure. 15 Principal stresses

The corresponding maximum displacement for a D/H, and maximum octahedral stress show in Table 2.

Table. 2 Maximum displacement and maximum octahedral stress

Combination D,H	Maximum Total Displacements (m)	Octahedral stresses (kPa)	H_c/H^* (%)
D=12m,H=20m	-0.0418	528.66	0.75
D=12m,H=24m	-0.0423	685.92	0.71
D=12m,H=28m	-0.0428	846.50	0.75
D=12m,H=32m	-0.0433	1018.28	0.78
D=14m,H=20m	-0.0415	601.45	0.65
D=14m,H=24m	-0.0418	782.05	0.71
D=14m,H=28m	-0.0423	967.66	0.75
D=14m,H=32m	-0.0427	1171.31	0.78
D=16m,H=20m	-0.0412	667.77	0.65
D=16m,H=24m	-0.0414	870.74	0.71
D=16m,H=28m	-0.0417	1081.06	0.75
D=16m,H=32m	-0.0419	1315.52	0.78

Hc: Critical depth where the maximum octahedral shear stress occurs

CONCLUSIONS

A proper assessment of seismic-induced stresses developed in an shaft during an strong ground motion is a key element during the design of hydraulic underground strategic infrastructure. In particular, in soft clay deposits it can be seen that the shaft behaves like a rigid body due to is higher relative stiffness with respect to the surrounding soil. Thus, important relative movements are generated between the soil and structure, which in turn lead to stresses in the shaft. The maximum octahedral stress is presented at an average depth of 0.73 times the shaft high H, ranging from 0.65 to 0.78. The maximum computed total shaft displacements is about -0.0433m, and occurs for a ration H/D of 2.66. The maximum computed octahedral stress is 1315.52 kPa and occurs for H/D of 2.0. Further studies will allow to establish a relationship among the more relevant variables controlling the seismic response of an shaft.

REFERENCES

Abrahamson, N. A., 2000. State of the practice of seismic hazard evaluation. Proceedings of GeoEng 2000, Melbourne, 19-24 November, Vol. 1, pp. 659-685

A.Amorosi, D.Boldini. Numerical modelling of the transverse dynamic behavior of circular tunnels in clayey soils. Soil Dynamics and Earthquake Engineering 2008; DOI: 10.1016/j.soildyn.2008.12.009.

Safak E. Local site effects and dynamic soil behavior. Soil Dynamics and Earthquake Engineering 2001; 21:453–458.

Darendeli MB, Stokoe KH. Development of a new family of normalized modulus reduction and material damping curves. Geotechnical Engineering Report GD01-1, University of Texas at Austin, Austin, 2001.

Dobry R, Vucetic M. Dynamic properties and seismic response of soft clay deposits. International Symposium Geotechnical Engineering of Soft Soils, vol. 2, Mexico City, 1987; 51–87.

Rosenblueth E. Theory of the seismic design over soft deposits .Ediciones ICA: México B, 14; 1952 [in Spanish].

Idriss IM, Seed HB. Seismic response of horizontal soil layers. J Soil Mech Found ASCE 1968;94(SM4):1003–31.

Romo MP, Jaime A. Características dinámicas de las arcillas del Valle de México y análisis de respuesta de sitio, Reporte Interno, Instituto de Ingeniería, UNAM; 1986.

Seed RB, Dickenson SE, Mok CM. Site effects on strong shaking and seismic risk: Recent developments and their impact on seismic design codes and practice. In: Proceedings of structure congress XII, ASCE, vol. 1; 1994. p. 573-8.

Schnabel PB, Lysmer J, Seed HB. SHAKE: a computer program for earthquake responser analysis of horizontally latered Sites; College of Engineering, Report No. EERC 72-12, University of Berkeley, CA, 1972.

Ovando, E. y Romo, M. P., 1991. Estimación de la velocidad de ondas S en la arcilla de la ciudad de México con ensayos de cono, Revista Sismodinámica, 2, 107 123

Lilhanand K. y Tseng W. S., 1988. Development and application of realistic earthquake time histories compatible with multiple damping response spectra. Proceedings of the 9th World Conference on Earthquake Engineering, Tokyo, Japan, Vol. II, pp 819-824

Fabio Sabetta, Antonio Lucantoni, Hilmar Bungum, Julian J. Bommer, 2005. Sensitivity of PSHA results to ground motion prediction relations and logic-tree weights. Soil Dynamics and Earthquake Engineering 2005; 25:317–329.

R. Romeo,, A. Prestininzi. Probabilistic versus deterministic seismic hazard analysis: an integrated approach for siting problems. Soil Dynamics and Earthquake Engineering 2000; 20:75–84.

Wang J N. Seismic design of tunnels: a state – of – the - art approach. Monograph 7. NewYork, Parsons, Brinckerhoff: Quade & Diuglas Inc.; 1993

Mayoral, J. M., Romo, M. P. y Osorio, L., 2008a. Seismic parameters characterization at Texcoco lake, Mexico. Soil Dynamics and Earthquake Engineering, Volume 28, Issue 7, Pages 507-521, July.

Mayoral, J. M. y Osorio, L., 2013. Seismic microzonation for the northeast Texcoco lake area, Mexico. Soil Dynamics and Earthquake Engineering, Volume 48, Issue 7, Pages 252-266, Jan.

Mayoral, J. M. y Castañon E., 2014. Informe interno del Instituto de Ingeniería, UNAM (Spanish)